AIMS Mathematics, 11(4): 11410–11436.
DOI: 10.3934/math.2026470
Received: 19 January 2026
Revised: 04 April 2026
Accepted: 13 April 2026
Published: 24 April 2026

https://www.aimspress.com/journal/Math

Research article

On a unified Yosida inclusion problem and its computational implications

Mohd. Falahat Khan[1], **Syed Shakaib Irfan**[1], **Iqbal Ahmad**[2,*], **and Ibrahim Karahan**[3]

[1] Department of Mathematics, Aligarh Muslim University, Aligarh 202002, India
[2] Department of Mechanical Engineering, College of Engineering, Qassim University, Saudi Arabia
[3] Department of Mathematics, Faculty of Science, Erzurum Technical University, Erzurum, Turkey

* **Correspondence:** Email: i.ahmad@qu.edu.sa.

Abstract: This paper introduced and considered the Yosida inclusion problem, which is a unified model arising from the monotone inclusion, fixed point, and Cayley inclusion problems. By using the Yosida operator as a regularized and generically differentiable approximation of a maximal monotone operator for solving the Yosida inclusion problem we devised efficient and stable iterative algorithms instead of direct resolvent computation. This approach offers both theoretical and computational advantages for solving complex mathematical operator inclusion problems in Hilbert spaces. We demonstrated that the sequence generated by the proposed inertial S-iteration converges strongly. A theoretical example and an application were also presented to illustrate the effectiveness of the proposed algorithms.

Keywords: algorithms; image restoration; mathematical operator; optimization; monotone inclusion
Mathematics Subject Classification: 47H05, 47H09, 47J22, 49J40

1. Introduction

The variational inclusion problem serves as a broad mathematical framework that encompasses numerous fundamental models, including variational inequalities, equilibrium problems, and optimization issues. Over the past decades, extensive research has been devoted to developing iterative algorithms for solving such problems due to their wide applicability in applied mathematics, engineering, and optimization issues. For more details, see [1, 2].

Similarly, fixed point theory has evolved as a powerful tool in nonlinear analysis, providing iterative schemes for approximating solutions of mathematical operator equations. To establish a unifying link between these two, the Cayley inclusion problem [3] was proposed, wherein the Cayley transform of the resolvent operator bridges monotone inclusions and fixed point issues. This connection allows

the use of resolvent-based transformations to analyze and compute common solutions within a unified theoretical setting.

Let $\mathscr{T}$ be a nonempty closed convex subset of a real Hilbert space $\mathcal{X}$ equipped with inner product $\langle\cdot,\cdot\rangle$ and induced norm $\|\cdot\|$. The variational inclusion problem [4, 5] is to find $s \in \mathcal{X}$ such that $0 \in (\mathscr{A} + \mathscr{M})s$, where $\mathscr{A} : \mathcal{X} \to \mathcal{X}$ is a single-valued operator and $\mathscr{M} : \mathcal{X} \to 2^{\mathcal{X}}$ is a multivalued operator. If $\mathscr{A} \equiv 0$, then the problem reduces to the monotone inclusion problem: find $s \in \mathcal{X}$ such that $0 \in \mathscr{M}(s)$, which has been investigated by several authors [6, 7].

In connection with the monotone inclusion framework, the fixed point problem associated with a nonexpansive mapping $\mathcal{K} : \mathcal{X} \to \mathcal{X}$ focuses on finding

$$s \in \mathcal{X} \text{ such that } \mathcal{K}(s) = s, \tag{1.1}$$

where Π denotes the solution set of the fixed point problem. This formulation provides a unified and systematic approach to investigating a wide range of nonlinear problems, with significant applications in optimization, functional analysis, and other areas of applied mathematics [8, 9].

In this direction, Dar et al. [10] introduced the Cayley inclusion problem defined by:

$$\text{Find } s \in \mathcal{X} \text{ such that } 0 \in (\mathscr{C} + \mathscr{M})s,$$

where $\mathscr{M} : \mathcal{X} \to 2^{\mathcal{X}}$ is a maximal monotone mapping and $\mathscr{C} = 2\mathcal{R}^{\mathscr{M}}_{\mathcal{I},\eta} - \mathcal{I}$ is the Cayley operator associated with the resolvent mapping $\mathcal{R}^{\mathscr{M}}_{\mathcal{I},\eta}$. This generalization elegantly unites fixed point and monotone inclusion frameworks through the use of resolvent-based operators.

Dar et al. proposed a projection-type iterative scheme:

$$\begin{aligned} u_0 &\in \mathscr{T}, \\ y_m &= \mathscr{R}^{\mathscr{C}+\mathscr{M}}_{\eta}(u_m), \\ u_{m+1} &= \eta_m x + (1-\eta_m)\mathcal{K}(y_m), \quad m \geq 1, \end{aligned}$$

where $\{\eta_m\} \subset (0, 1)$. Under appropriate assumptions, they established the convergence of the generated sequence to a common solution of fixed point problem (1.1) and the Cayley inclusion problem.

Later, Husain et al. [11] proposed an inertial modified S-iteration algorithm that incorporates an inertial term to accelerate convergence and improve stability, building upon the classical S-iteration scheme studied in [12, 13]. Their iterative process is given by

$$\begin{aligned} z_m &= u_m + \vartheta_m(u_m - u_{m-1}), \\ y_m &= (1-\zeta_m)z_m + \zeta_m\mathcal{K}(z_m), \\ u_{m+1} &= (1-\eta_m)\mathcal{K}(y_m) + \eta_m\mathscr{R}^{\mathscr{C}+\mathscr{M}}_{\eta}(y_m), \quad m \geq 1, \end{aligned}$$

where $\{\vartheta_m\}$, $\{\zeta_m\}$, and $\{\eta_m\}$ are sequences in $(0, 1)$.

Motivated by these developments, we introduce a new and more general framework called the Yosida inclusion problem, formulated as:

$$\text{Find } s \in \mathcal{X} \text{ such that } 0 \in (\mathcal{J}^{\mathscr{M}}_{\mathcal{I},\eta} + \mathscr{M})s, \tag{1.2}$$

where

$$\mathcal{J}^{\mathscr{M}}_{\mathcal{I},\eta} = \frac{1}{\eta}[\mathcal{I} - \mathcal{R}^{\mathscr{M}}_{\mathcal{I},\eta}]$$

denotes the Yosida operator associated with the maximal monotone operator $\mathscr{M}$.

The motivation behind the Yosida inclusion problem lies in its regularized and smooth structure, which offers notable computational advantages. The Yosida approximation is single-valued, Lipschitz continuous, and easily computable, allowing the development of efficient iterative and gradient-type algorithms. Consequently, the Yosida inclusion problem can be viewed as a useful analytical tool and a numerically stable framework that builds on and extends the classical monotone inclusion problem and the Cayley inclusion problem.

In summary, letting $\mathcal{J}^{\mathscr{M}}_{\mathcal{I},\eta}(s) = \mathcal{J}(s)$, the Yosida inclusion problem can equivalently be expressed as

$$0 \in \mathcal{J}(s) + \mathscr{M}(s), \tag{1.3}$$

and the solution set of the Yosida inclusion problem is denoted by Ψ.

2. Basic results

The fundamental results in this section provide the analytical foundation for the subsequent developments, ensuring the theoretical consistency of the main theorems and the iterative algorithms for solving variational inclusion and fixed point problems in Hilbert spaces.

Definition 2.1. *A mapping $\mathcal{T} : \mathcal{X} \to \mathcal{X}$ is said to be:*

(i) monotone if

$$\langle \mathcal{T}(x) - \mathcal{T}(y), x - y\rangle \geq 0 \quad \forall x, y \in \mathcal{X};$$

(ii) nonexpansive if

$$\|\mathcal{T}(x) - \mathcal{T}(y)\| \leq \|x - y\| \quad \forall x, y \in \mathcal{X};$$

(iii) Lipschitz continuous for constant $L > 0$ if

$$\|\mathcal{T}(x) - \mathcal{T}(y)\| \leq L\|x - y\| \quad \forall x, y \in \mathcal{X}.$$

Now, letting $\mathscr{M} : \mathcal{X} \to 2^{\mathcal{X}}$ be a multivalued mapping with $D(M) = X$, we say that $\mathscr{M}$ is monotone, if for all $x, y \in \mathcal{X}$, there exist $x_1 \in \mathscr{M}(x)$ and $y_1 \in \mathscr{M}(y)$ such that

$$\langle x - y, x_1 - y_1\rangle \geq 0,$$

and maximal monotone if $\mathscr{M}$ is monotone and $(\mathcal{I} + \lambda\mathscr{M})(\mathcal{X}) = \mathcal{X}$ for all $\lambda > 0$, where $\mathcal{I}$ denotes the identity mapping on $\mathcal{X}$.

Definition 2.2. *Let $\mathscr{M} : \mathcal{X} \to 2^{\mathcal{X}}$ be a multivalued maximal monotone mapping. Then the resolvent operator $\mathcal{R}^{\mathscr{M}}_{\mathcal{I},\eta} : \mathcal{X} \to \mathcal{X}$ is defined as*

$$\mathcal{R}^{\mathscr{M}}_{\mathcal{I},\eta}(x) = (\mathcal{I} + \eta\mathscr{M})^{-1}(x), \quad \forall x \in \mathcal{X}, \ \ \eta > 0.$$

Definition 2.3. *Let $\mathscr{M} : \mathcal{X} \to 2^{\mathcal{X}}$ be a multivalued maximal monotone mapping and let $\mathcal{R}^{\mathscr{M}}_{\mathcal{I},\eta}$ be the resolvent operator associated with $\mathscr{M}$. Then the Yosida operator is defined as*

$$\mathcal{J}^{\mathscr{M}}_{\mathcal{I},\eta}(x) = \frac{1}{\eta}\left[\mathcal{I} - \mathcal{R}^{\mathscr{M}}_{\mathcal{I},\eta}\right](x), \quad \forall x \in \mathcal{X}.$$

Lemma 2.1. *The resolvent operator $\mathcal{R}^{\mathscr{M}}_{\mathcal{I},\eta}$ is single-valued and satisfies the following properties:*

(i) nonexpansive

$$\|\mathcal{R}^{\mathscr{M}}_{\mathcal{I},\eta}(x) - \mathcal{R}^{\mathscr{M}}_{\mathcal{I},\eta}(y)\| \leq \|x - y\| \quad \forall x, y \in \mathcal{X};$$

(ii) 1*-inversely strongly monotone*

$$\|\mathcal{R}^{\mathscr{M}}_{\mathcal{I},\eta}(x) - \mathcal{R}^{\mathscr{M}}_{\mathcal{I},\eta}(y)\|^2 \leq \langle x - y, \mathcal{R}^{\mathscr{M}}_{\mathcal{I},\eta}(x) - \mathcal{R}^{\mathscr{M}}_{\mathcal{I},\eta}(y)\rangle \quad \forall x, y \in \mathcal{X}.$$

Proof. Let $x, y \in \mathcal{X}$ and define

$$p = \mathcal{R}^{\mathscr{M}}_{\mathcal{I},\eta}(x), \qquad q = \mathcal{R}^{\mathscr{M}}_{\mathcal{I},\eta}(y).$$

Then, by the definition of the resolvent operator, we have

$$\frac{x - p}{\eta} \in \mathscr{M}(p) \quad \text{and} \quad \frac{y - q}{\eta} \in \mathscr{M}(q).$$

Let

$$u = \frac{x - p}{\eta}, \qquad v = \frac{y - q}{\eta}.$$

Since $\mathscr{M}$ is monotone, and substituting the values of u and v, we obtain

$$\left\langle \frac{x - p}{\eta} - \frac{y - q}{\eta},\ p - q \right\rangle \geq 0,$$

which implies that

$$\begin{aligned} \langle x - y,\ p - q\rangle &\geq \langle p - q,\ p - q\rangle \\ &= \|p - q\|^2. \end{aligned}$$

Hence, we obtain

$$\|\mathcal{R}^{\mathscr{M}}_{\mathcal{I},\eta}(x) - \mathcal{R}^{\mathscr{M}}_{\mathcal{I},\eta}(y)\|^2 \leq \langle x - y, \mathcal{R}^{\mathscr{M}}_{\mathcal{I},\eta}(x) - \mathcal{R}^{\mathscr{M}}_{\mathcal{I},\eta}(y)\rangle.$$

Therefore, $\mathcal{R}^{\mathscr{M}}_{\mathcal{I},\eta}$ is 1-inverse strongly monotone. Now, by the Cauchy–Schwarz inequality, we get

$$\|\mathcal{R}^{\mathscr{M}}_{\mathcal{I},\eta}(x) - \mathcal{R}^{\mathscr{M}}_{\mathcal{I},\eta}(y)\| \leq \|x - y\|.$$

Hence, $\mathcal{R}^{\mathscr{M}}_{\mathcal{I},\eta}$ is nonexpansive. □

Lemma 2.2. *[14] Let $\mathcal{X}$ be a real Hilbert space and let $\mathscr{M} : \mathcal{X} \to 2^{\mathcal{X}}$ be a maximal monotone operator. Then the Yosida operator has the following properties:*

(i) $\mathcal{J}^{\mathscr{M}}_{\mathcal{I},\eta}$ *is* $\frac{1}{\eta}$*-Lipschitz continuous, that is,*

$$\|\mathcal{J}^{\mathscr{M}}_{\mathcal{I},\eta}(x) - \mathcal{J}^{\mathscr{M}}_{\mathcal{I},\eta}(y)\| \leq \frac{1}{\eta}\|x - y\|, \qquad \forall x, y \in \mathcal{X};$$

(ii) $\mathcal{J}^{\mathscr{M}}_{\mathcal{I},\eta}$ *is* η*-inverse strongly monotone, that is,*

$$\langle \mathcal{J}^{\mathscr{M}}_{\mathcal{I},\eta}(x) - \mathcal{J}^{\mathscr{M}}_{\mathcal{I},\eta}(y),\ x - y\rangle \geq \eta\|\mathcal{J}^{\mathscr{M}}_{\mathcal{I},\eta}(x) - \mathcal{J}^{\mathscr{M}}_{\mathcal{I},\eta}(y)\|^2$$

for all $x, y \in \mathcal{X}$.

Lemma 2.3. *[15] Let $\mathcal{X}$ be a real Hilbert space. Then, for any $x, y \in \mathcal{X}$, the following relations are satisfied:*

(i) $\|x + y\|^2 \leq \|x\|^2 + 2\langle y,\ x + y\rangle$*;*

(ii) $\|x - y\|^2 = \|x\|^2 - \|y\|^2 - 2\langle x - y,\ y\rangle$*;*

(iii) For every $\alpha \in \mathbb{R}$,

$$\|\alpha x + (1 - \alpha)y\|^2 = \alpha\|x\|^2 + (1 - \alpha)\|y\|^2 - \alpha(1 - \alpha)\|x - y\|^2.$$

Lemma 2.4. *[16] Let $\mathscr{M} : \mathcal{X} \to 2^{\mathcal{X}}$ be a maximal monotone mapping and $\mathscr{A} : \mathcal{X} \to \mathcal{X}$ be a Lipschitz continuous and monotone mapping. Then a mapping $\mathscr{M} + \mathscr{A} : \mathcal{X} \to 2^{\mathcal{X}}$ is a maximal monotone mapping.*

In view of the above lemma, we have that $\mathcal{J} + \mathscr{M} : \mathcal{X} \to 2^{\mathcal{X}}$ is a maximal monotone mapping, so we can define a new resolvent operator as follows.

Definition 2.4. *Let $\mathscr{M} : \mathcal{X} \to 2^{\mathcal{X}}$ be a maximal monotone mapping and $\mathcal{J} : \mathcal{X} \to \mathcal{X}$ be a Yosida operator possessing the Lipschitz continuity property so that $\mathcal{J} + \mathscr{M} : \mathcal{X} \to 2^{\mathcal{X}}$ is also a maximal monotone mapping. So, the resolvent operator associated with $\mathcal{J} + \mathscr{M}$ is*

$$\mathscr{R}_{\eta}^{\mathcal{J}+\mathscr{M}}(x) = \left[\mathcal{I} + \eta(\mathcal{J} + \mathscr{M})\right]^{-1}(x).$$

Remark 2.1. *The resolvent operator $\mathscr{R}_{\eta}^{\mathcal{J}+\mathscr{M}}$ is nonexpansive and* 1*-inverse strongly monotone.*

Lemma 2.5. *(*Opial's property*) Let $\mathcal{X}$ be a Hilbert space. Then for each sequence $\{u_m\}$ in $\mathcal{X}$ converging weakly to a point $s \in \mathcal{X}$, one has*

$$\liminf_{m\to\infty} \|u_m - s\| < \liminf_{m\to\infty} \|u_m - t\|, \quad \forall\, t \in \mathcal{X},\ t \neq s.$$

Lemma 2.6. *[17] Let $\{a_m\}, \{b_m\}$, and $\{c_m\}$ be sequences in $[0, \infty)$ satisfying $a_{m+1} \leq a_m + c_m(a_m - a_{m-1}) + b_m$, $\forall m \geq 1$, provided $\sum_{m=1}^{\infty} b_m < \infty$ with $0 \leq c_m \leq \alpha < 1$, $\forall m \geq 1$. Then the following conditions hold:*

(i) $\sum_{m\geq 1}[a_m - a_{m-1}]_+ < \infty$*, where* $[\check{t}]_+ = max[\check{t}, 0]$.

(ii) $\exists\, a^* \in [0,\infty)$ *such that* $\lim_{m\to\infty} a_m = a^*$.

Definition 2.5. *[18] Let* $\mathscr{T}$ *be a subset of a metric space* $(X,\check{d})$*. A mapping* $\mathcal{K}:\mathscr{T}\to\mathscr{T}$ *is semi-compact if for each sequence* $\{u_m\}$ *in* $\mathscr{T}$ *with* $\lim_{m\to\infty}(\check{d}(u_m,\mathcal{K}(u_m)))=0$*, there exists a subsequence* $\{u_{m_k}\}$ *of* $\{u_m\}$ *such that* $u_{m_k}\to s\in\mathscr{T}$.

Definition 2.6. *[18] Let* $\mathscr{T}$ *be a nonempty, closed, and convex subset of a real Hilbert space* $\mathcal{X}$*. The operators* $\mathcal{K}$ *and* $\mathscr{R}^{\mathcal{J}+\mathscr{M}}$ *defined on* $\mathscr{T}$ *are said to satisfy the Condition (B), if there exists a non-decreasing function* $\check{k}:[0,\infty)\to[0,\infty)$ *such that* $\check{k}(0)=0$ *and* $\check{k}(\check{s})>0$ *for every* $\check{s}>0$*, and the inequality*

$$\max\Big\{\|\check{s}-\mathcal{K}(\check{s})\|,\ \|\check{s}-\mathscr{R}^{\mathcal{J}+\mathscr{M}}(\check{s})\|\Big\}\geq\check{k}\Big(\check{d}(\check{s},\Gamma)\Big),\quad\forall\,\check{s}\in\mathscr{T},$$

holds, where $\Gamma=\Psi\cap\Pi$*. Here,*

$$\check{d}(\check{s},\Gamma)=\inf_{y\in\Gamma}\|\check{s}-y\|$$

represents the distance from the point $\check{s}$ *to the set* Γ.

Lemma 2.7. *[1] Let* $\mathcal{X}$ *be a real Hilbert space, and let* $\{\eta_m\}$ *be a sequence in* $[\nu,1-\nu]$*, where* $\nu\in(0,1)$*. Suppose that the sequences* $\{u_m\}$ *and* $\{z_m\}$ *in* $\mathcal{X}$ *satisfy the following conditions:*

(i) $\liminf_{m\to\infty}\|u_m\|\leq\varsigma$,

(ii) $\liminf_{m\to\infty}\|z_m\|\leq\varsigma$,

(iii) $\liminf_{m\to\infty}\|\eta_m u_m+(1-\eta_m)z_m\|=\varsigma$*, for some* $\varsigma\geq 0$.

Then it follows that $\liminf_{m\to\infty}\|u_m-z_m\|=0$.

Lemma 2.8. *[19] Suppose* $\mathcal{X}$ *is a real Hilbert space and let* $\{u_m\}$ *be a sequence in* $\mathcal{X}$*. Consider* $\check{s}_1,\check{s}_2\in\mathcal{X}$ *to be such that the limits* $\lim_{m\to\infty}\|u_m-\check{s}_1\|$ *and* $\lim_{m\to\infty}\|u_m-\check{s}_2\|$ *exist. If* $\{u_{m_k}\}$ *and* $\{u_{m_j}\}$ *are two subsequences of* $\{u_m\}$ *converging to* $\check{s}_1$ *and* $\check{s}_2$*, respectively, then* $\check{s}_1=\check{s}_2$.

Lemma 2.9. *[14] Let* $\mathscr{T}$ *be a nonempty subset of a real Hilbert space* $\mathcal{X}$*, and let* u_m *be a sequence in* $\mathcal{X}$ *satisfying the following conditions:*

(i) For every $s\in\mathscr{T}$*, the limit* $\lim_{m\to\infty}\|u_m-s\|$ *exists.*

(ii) Every weak cluster point of u_m *belongs to* $\mathscr{T}$.

Then the sequence $\{u_m\}$ *converges weakly to some point* $s\in\mathscr{T}$.

Lemma 2.10. *[14] Let* $\mathscr{T}$ *be a nonempty, closed, and convex subset of a real Hilbert space* $\mathcal{X}$*, and let* $\mathcal{K}:\mathscr{T}\to\mathcal{X}$ *be a nonexpansive operator. Assume that* $\{u_m\}$ *is a sequence in* $\mathscr{T}$ *that converges weakly to some point* $x\in\mathcal{X}$*. If*

$$\lim_{m\to\infty}\|\mathcal{K}(u_m)-u_m\|=0,$$

then x *is a fixed point of* $\mathcal{K}$*, that is,* $x\in\Pi$.

3. Main results

In this section, we present the modified inertial S-iteration method to solve the common solution of the fixed point problem (1.1) and the Yosida inclusion problem (1.3). Let the solution set of fixed point problem be denoted by Π and the solution set of Yosida inclusion problem by Ψ. We assume that $\Gamma = \Pi \cap \Psi \neq \emptyset$ and, in order to establish the convergence of the iterative sequences generated by the proposed scheme, we adopt the following set of assumptions.

(H1) $\sum_{m=1}^{\infty} \theta_m < \infty$ and $\{\theta_m\} \subset [0, 1]$.

(H2) $\{\tau_m\}, \{\eta_m\} \subset [\varsigma, 1 - \varsigma]$, for some $\varsigma \in (0, 0.5)$.

(H3) $\{\mathcal{K}(y_m) - y_m\}, \{\mathcal{K}(y_m) - s\}$ are bounded.

(H4) $\{\mathscr{R}_{\eta}^{\mathcal{J}+\mathscr{M}}(y_m) - y_m\}, \{\mathscr{R}_{\eta}^{\mathcal{J}+\mathscr{M}}(y_m) - s\}$ are bounded for any $s \in \Gamma$.

Algorithm 1 Modified Inertial S-iteration

Let $u_0 \in \mathcal{X}$. For $m \geq 0$, define the sequences $\{u_m\}, \{y_m\}, \{z_m\}$ by

$$y_m = u_m + \theta_m(u_m - u_{m-1}), \tag{3.1}$$

$$z_m = (1 - \tau_m)y_m + \tau_m \mathcal{K}(y_m), \tag{3.2}$$

$$u_{m+1} = (1 - \eta_m)\mathcal{K}(y_m) + \eta_m \mathscr{R}_{\eta}^{\mathcal{J}+\mathscr{M}}(z_m), \tag{3.3}$$

where $\mathcal{K} : \mathcal{X} \to \mathcal{X}$ and $\mathscr{R}_{\eta}^{\mathcal{J}+\mathscr{M}} : \mathcal{X} \to \mathcal{X}$ are nonexpansive mappings, and the parameters satisfy

(i) $\theta_m \in [0, 1]$ and $\sum_{m=1}^{\infty} \theta_m < \infty$,

(ii) $\{\eta_m\}, \{\tau_m\} \subset [\varsigma, 1 - \varsigma]$ for some $\varsigma \in (0, 0.5)$.

Lemma 3.1. *For $\eta > 0$, $x \in \mathcal{X}$ is the solution of Yosida inclusion problem* (1.3) *if and only if*

$$x = \mathscr{R}_{\eta}^{\mathcal{J}+\mathscr{M}}(x). \tag{3.4}$$

Proof. Suppose x is the solution of (1.3). Then

$$0 \in (\mathcal{J} + \mathscr{M})(x).$$

Multiplying by $\eta > 0$ and adding x, we obtain

$$x \in [\mathcal{I} + \eta(\mathcal{J} + \mathscr{M})](x).$$

Therefore, we get

$$x = [\mathcal{I} + \eta(\mathcal{J} + \mathscr{M})]^{-1}(x) = \mathscr{R}_{\eta}^{\mathcal{J}+\mathscr{M}}(x).$$

Conversely, if $x = \mathscr{R}_{\eta}^{\mathcal{J}+\mathscr{M}}(x)$, then

$$x \in [\mathcal{I} + \eta(\mathcal{J} + \mathscr{M})](x),$$

which implies $0 \in (\mathcal{J} + \mathscr{M})(x)$. Hence x is the solution of (1.3). □

Theorem 3.1. *Let $\mathcal{X}$ be a real Hilbert space endowed with the Opial property and $\mathscr{M} : \mathcal{X} \rightrightarrows \mathcal{X}$ be a multivalued maximal monotone mapping. Let $\mathcal{J} : \mathcal{X} \to \mathcal{X}$ be the Yosida operator, which is Lipschitz continuous. $\mathcal{J} + \mathscr{M} : \mathcal{X} \rightrightarrows \mathcal{X}$ is a maximal monotone mapping and $\mathcal{K}, \mathscr{R}_{\eta}^{\mathcal{J}+\mathscr{M}} : \mathcal{X} \to \mathcal{X}$ are nonexpansive mappings. Let all conditions $(H_1) - (H_4)$ hold, and then*

(i) $\lim_{m\to\infty} \|u_m - s\|$ *exists.*

(ii) $\lim_{m\to\infty} \|u_m - \mathcal{K}(u_m)\| = \lim_{m\to\infty} \|u_m - \mathscr{R}_{\eta}^{\mathcal{J}+\mathscr{M}}(u_m)\| = 0.$

Moreover, the sequence generated by Algorithm 1 converges weakly to a common fixed point of $\Gamma = \Pi \cap \Psi$.

Proof. **Step 1:** Let $s \in \Gamma$. We aim to show that the sequence $\|u_m - s\|$ converges. Using the nonexpansive property of $\mathcal{K}$, we obtain

$$\begin{aligned} \|z_m - s\| &= \left\|(1-\tau_m)y_m + \tau_m \mathcal{K}(y_m) - s\right\| \\ &\leq (1-\tau_m)\|y_m - s\| + \tau_m\|\mathcal{K}(y_m) - s\| \\ &\leq \|y_m - s\|. \end{aligned} \tag{3.5}$$

Now,

$$\begin{aligned} \|u_{m+1} - s\| &= \left\|(1-\eta_m)\mathcal{K}(y_m) + \eta_m \mathscr{R}_{\eta}^{\mathcal{J}+\mathscr{M}}(z_m) - s\right\| \\ &\leq (1-\eta_m)\|\mathcal{K}(y_m) - s\| + \eta_m\|\mathscr{R}_{\eta}^{\mathcal{J}+\mathscr{M}}(z_m) - s\|. \end{aligned}$$

Using the nonexpansive properties of $\mathcal{K}$, $\mathscr{R}_{\eta}^{\mathcal{J}+\mathscr{M}}$, and (3.5), we get

$$\|u_{m+1} - s\| \leq \|y_m - s\|. \tag{3.6}$$

From condition (H3), we have

$$\begin{aligned} \|y_m - s\| &= \|y_m - \mathcal{K}(y_m) + \mathcal{K}(y_m) - s\| \\ &\leq \|\mathcal{K}(y_m) - y_m\| + \|\mathcal{K}(y_m) - s\| \\ &\leq M_1 + M_2 = M. \end{aligned}$$

For some $M \in [0, \infty)$, which shows that $\{y_m\}$ is bounded, and from (3.6), we say that $\{u_m\}$ is bounded. Now,

$$\begin{aligned} \|y_m - s\|^2 &= \|(u_m + \theta_m(u_m - u_{m-1})) - s\|^2 \\ &= \|(1+\theta_m)(u_m - s) - \theta_m(u_{m-1} - s)\|^2. \end{aligned}$$

Using Lemma 2.3, we have

$$\|y_m - s\|^2 = (1+\theta_m)\|u_m - s\|^2 - \theta_m\|u_{m-1} - s\|^2 + \theta_m(1+\theta_m)\|u_m - u_{m-1}\|^2. \tag{3.7}$$

From Eq (3.6), we get

$$\|u_{m+1} - s\|^2 \leq (1+\theta_m)\|u_m - s\|^2 - \theta_m\|u_{m-1} - s\|^2 + \theta_m(1+\theta_m)\|u_m - u_{m-1}\|^2.$$

Let $\xi_m = \|u_m - s\|^2$. Then the above equation becomes

$$\xi_{m+1} \leq \xi_m + \theta_m(\xi_m - \xi_{m-1}) + \theta_m(1+\theta_m)\|u_m - u_{m-1}\|^2. \tag{3.8}$$

Using condition (H1),

$$\sum\nolimits_{m=1}^{\infty}\theta_m(1-\theta_m)\|u_m - u_{m-1}\|^2 \leq \theta_m(1-\theta_m)(2M)^2 < \infty. \tag{3.9}$$

Using (3.8) and (3.9), we obtain

$$\xi_{m+1} \leq \xi_m + \theta_m(\xi_m - \xi_{m-1}) + b_m.$$

Since $0 \leq \theta_m \leq \alpha < 1$ for all $m \geq 1$ and $\sum_{m=1}^{\infty} b_m < \infty$, the conditions of Lemma 2.6 are satisfied. Hence, by Lemma 2.6, there exists $a^* \in [0, \infty)$ such that

$$\lim_{m\to\infty} \xi_m = a^*.$$

Consequently, the limit $\lim_{m\to\infty} \|u_m - s\|^2$ exists and therefore $\lim_{m\to\infty} \|u_m - s\|$ exists.

Step 2: Set $\lim_{m\to\infty} \|u_m - s\| = \varrho$.

Now, nonexpansivness of $\mathcal{K}$ and $\mathscr{R}_{\eta}^{\mathcal{J}+\mathscr{M}}$, we have

$$\|u_m - \mathcal{K}(u_m)\| \leq 2\|u_m - s\|.$$

Also,

$$\|u_m - \mathscr{R}_{\eta}^{\mathcal{J}+\mathscr{M}}(u_m)\| \leq 2\|u_m - s\|.$$

If $\varrho = 0$, then we get $\|u_m - \mathcal{K}(u_m)\| \to 0$ and $\|u_m - \mathscr{R}_{\eta}^{\mathcal{J}+\mathscr{M}}(u_m)\| \to 0$. Now consider $\varrho > 0$. If $\sum_{m=1}^{\infty}\theta_m < \infty$, then $\lim_{m\to\infty} \theta_m = 0$ and by (3.7), we have

$$\begin{aligned}\lim_{m\to\infty} \|y_m - s\|^2 &= \lim_{m\to\infty}\left[(1+\theta_m)\|u_m - s\|^2 - \theta_m\|u_{m-1} - s\|^2 + \theta_m(1+\theta_m)\|u_m - u_{m-1}\|^2\right] \\ &= \lim_{m\to\infty} \|u_m - s\|^2 = \varrho^2.\end{aligned}$$

Therefore, $\lim_{m\to\infty} \|y_m - s\| = \varrho$ and, from (3.5), we have

$$\limsup_{m\to\infty} \|z_m - s\| \leq \limsup_{m\to\infty} \|y_m - s\| = \varrho.$$

In the following way, we show that

$$\liminf_{m\to\infty} \|z_m - s\| \geq \varrho.$$

By employing the nonexpansive properties of $\mathcal{K}$ and $\mathscr{R}_{\eta}^{\mathcal{J}+\mathscr{M}}$, together with Lemma 2.3, we obtain the following result.

$$\begin{aligned}
\|u_{m+1}-s\|^2 &= \left\|(1-\eta_m)\mathcal{K}(y_m)+\eta_m\mathscr{R}_{\eta}^{\mathcal{J}+\mathscr{M}}(z_m)-s\right\|^2\\
&\leq (1-\eta_m)\|\mathcal{K}(y_m)-s\|^2+\eta_m\left\|\mathscr{R}_{\eta}^{\mathcal{J}+\mathscr{M}}(z_m)-s\right\|^2\\
&\leq (1-\eta_m)\|\mathcal{K}(y_m)-\mathcal{K}(s)\|^2+\eta_m\left\|\mathscr{R}_{\eta}^{\mathcal{J}+\mathscr{M}}(z_m)-\mathscr{R}_{\eta}^{\mathcal{J}+\mathscr{M}}(s)\right\|^2\\
&\leq (1-\eta_m)\|y_m-s\|^2+\eta_m\|z_m-s\|^2. \qquad (3.10)
\end{aligned}$$

Rearranging (3.10) and the condition used in Algorithm 1, we have

$$\|y_m-s\|^2\leq\|z_m-s\|^2+\frac{1}{\eta_m}\Big(\|y_m-m\|^2+\|u_{m+1}-s\|^2\Big). \qquad (3.11)$$

From (3.6) and (3.11), we obtain the following relation:

$$\begin{aligned}
\liminf_{m\to\infty}\|z_m-s\|^2&\geq\varrho^2,\\
\liminf_{m\to\infty}\|z_m-s\|&\geq\varrho.
\end{aligned}$$

Therefore,

$$\varrho\leq\liminf_{m\to\infty}\|z_m-s\|\leq\limsup_{m\to\infty}\|z_m-s\|\leq\varrho,$$

and we get

$$\lim_{m\to\infty}\|z_m-s\|=\varrho.$$

Using the nonexpansiveness property of $\mathcal{K}$, we obtain

$$\begin{aligned}
\limsup_{m\to\infty}\|\mathcal{K}(y_m)-\mathcal{K}(s)\|&\leq\limsup_{m\to\infty}\|y_m-s\|,\\
\limsup_{m\to\infty}\|\mathcal{K}(y_m)-s\|&\leq\limsup_{m\to\infty}\|y_m-s\|\leq\varrho,\\
\lim_{m\to\infty}\|(1-\tau_m)(y_m-s)+\tau_m(\mathcal{K}(y_m)-s)\|&=\lim_{m\to\infty}\|z_m-s\|=\varrho. \qquad (3.12)
\end{aligned}$$

Now, using the nonexpansiveness property of $\mathscr{R}_{\eta}^{\mathcal{J}+\mathscr{M}}$, we obtain

$$\begin{aligned}
\|\mathscr{R}_{\eta}^{\mathcal{J}+\mathscr{M}}(z_m)-\mathscr{R}_{\eta}^{\mathcal{J}+\mathscr{M}}(s)\|&\leq\|z_m-s\|,\\
\limsup_{m\to\infty}\|\mathscr{R}_{\eta}^{\mathcal{J}+\mathscr{M}}(z_m)-\mathscr{R}_{\eta}^{\mathcal{J}+\mathscr{M}}(s)\|&\leq\limsup_{m\to\infty}\|z_m-s\|,\\
\limsup_{m\to\infty}\|\mathscr{R}_{\eta}^{\mathcal{J}+\mathscr{M}}(z_m)-s\|&\leq\limsup_{m\to\infty}\|z_m-s\|\leq\varrho,
\end{aligned}$$

$$\lim_{m\to\infty} \|(1-\eta_m)(\mathcal{K}(y_m)-s)+\eta_m(\mathscr{R}_\eta^{\mathcal{J}+\mathscr{M}}(z_m)-s)\| = \lim_{m\to\infty} \|u_{m+1}-s\| = \varrho. \tag{3.13}$$

Using Lemma 2.7 together with (3.12) and (3.13), we obtain

$$\lim_{m\to\infty} \|\mathcal{K}(y_m)-y_m\| \quad = 0, \tag{3.14}$$

$$\lim_{m\to\infty} \|\mathcal{K}(y_m)-\mathscr{R}_\eta^{\mathcal{J}+\mathscr{M}}(z_m)\| \quad = 0. \tag{3.15}$$

Using (3.1)−(3.3), we derive the following:

$$z_m - y_m = \tau_m(\mathcal{K}(y_m)-y_m),$$
$$y_m - u_m = \theta_m(u_m-u_{m-1}).$$

So, using (3.14) and (3.15),

$$0 \le \lim_{m\to\infty} \|z_m-y_m\| \le \lim_{m\to\infty} \|\mathcal{K}(y_m)-y_m\| = 0 \tag{3.16}$$

and

$$\lim_{m\to\infty} \|y_m-u_m\| = \lim_{m\to\infty} \theta_m\|u_m-u_{m-1}\| = 0. \tag{3.17}$$

Also,

$$\lim_{m\to\infty} \|\mathcal{K}(y_m)-u_m\| \le \lim_{m\to\infty} \|\mathcal{K}(y_m)-y_m\| + \lim_{m\to\infty} \theta_m\|u_m-u_{m-1}\| = 0. \tag{3.18}$$

Using (3.16)–(3.18) and the nonexpansiveness of $\mathcal{K}$ and $\mathscr{R}_\eta^{\mathcal{J}+\mathscr{M}}$, we have

$$\begin{aligned}
0 &\le \lim_{m\to\infty} \|\mathcal{K}(u_m)-u_m\| \\
&\le \lim_{m\to\infty} \left(\|\mathcal{K}(u_m)-\mathcal{K}(y_m)\| + \|\mathcal{K}(y_m)-u_m\|\right) \\
&\le \lim_{m\to\infty} \|u_m-y_m\| + \lim_{m\to\infty} \|\mathcal{K}(y_m)-u_m\| \\
&= 0
\end{aligned}$$

and

$$\begin{aligned}
0 &\le \lim_{m\to\infty} \left\|\mathscr{R}_\eta^{\mathcal{J}+\mathscr{M}}(u_m)-u_m\right\| \\
&\le \lim_{m\to\infty} \left\|\mathscr{R}_\eta^{\mathcal{J}+\mathscr{M}}(u_m)-\mathscr{R}_\eta^{\mathcal{J}+\mathscr{M}}(z_m)\right\| \\
&\quad + \lim_{m\to\infty} \left\|\mathscr{R}_\eta^{\mathcal{J}+\mathscr{M}}(z_m)-\mathcal{K}(y_m)\right\| + \lim_{m\to\infty} \|\mathcal{K}(y_m)-u_m\| \\
&\le \lim_{m\to\infty} \|u_m-z_m\| \\
&\le \lim_{m\to\infty} \|u_m-y_m\| + \lim_{m\to\infty} \|y_m-z_m\| \\
&= 0.
\end{aligned}$$

Therefore, we have

$$\lim_{m\to\infty} \|\mathcal{K}(u_m)-u_m\| = \lim_{m\to\infty} \|\mathscr{R}_\eta^{\mathcal{J}+\mathscr{M}}(u_m)-u_m\| = 0. \tag{3.19}$$

□

We have that $s \in \Phi$, $\lim_{m\to\infty} \|u_m - s\|$ exists, and $\{u_m\}$ is bounded. Let $\{u_{m_k}\}$ and $\{u_{m_j}\}$ be two sequences of $\{u_m\}$ that have weak limit z_1 and z_2, respectively. Using Eq (3.19), we have

$$\lim_{m\to\infty} \|\mathcal{K}(u_{m_k}) - u_{m_k}\| = \lim_{m\to\infty} \|\mathscr{R}_\eta^{\mathcal{J}+\mathscr{M}}(u_{m_k}) - u_{m_k}\| = 0,$$
$$\lim_{m\to\infty} \|\mathcal{K}(u_{m_j}) - u_{m_j}\| = \lim_{m\to\infty} \|\mathscr{R}_\eta^{\mathcal{J}+\mathscr{M}}(u_{m_j}) - u_{m_j}\| = 0.$$

Now, using Lemma 2.10, there exist two points z_1, z_2 such that $\mathcal{K}(z_1) = z_1, \mathcal{K}(z_2) = z_2$ and $\mathscr{R}_\eta^{\mathcal{J}+\mathscr{M}}(z_1) = z_1, \mathscr{R}_\eta^{\mathcal{J}+\mathscr{M}}(z_2) = z_2$. Therefore, using Step 1, we conclude that the following limit exist:

$$\lim_{m\to\infty} \|u_m - z_1\| \quad \text{and} \quad \lim_{m\to\infty} \|u_m - z_2\|,$$

and the subsequences $\{u_{m_k}\}$ and $\{u_{m_j}\}$ converge to z_1 and z_2, respectively. Using Lemma 2.8, we have $z_1 = z_2$. Hence, $\{u_m\}$ converges to a common fixed point of $\mathcal{K}$ and $\mathscr{R}_\eta^{\mathcal{J}+\mathscr{M}}$.

Using the relation established in Definition 2.6, the following theorem demonstrates that, under this relation, the iterative sequence generated by Algorithm 1 converges strongly to a common fixed point of the involved mappings.

Theorem 3.2. *Let $\mathcal{X}$ be a real Hilbert space, and let $\mathcal{K}, \mathscr{R}_\eta^{\mathcal{J}+\mathscr{M}} : \mathcal{X} \to \mathcal{X}$ be the non-expansive mapping such that $\Gamma = \Pi \cap \Psi$ and satisfies the relation of Definition 2.6. Then the sequence $\{u_m\}$ generated by Algorithm 1 converges strongly to a common fixed point of $\mathcal{K}$ and $\mathscr{R}_\eta^{\mathcal{J}+\mathscr{M}}$.*

Proof. Let $t \in \Gamma$. Then from Eq (3.8), we obtain

$$\begin{aligned}\|u_{m+1} - t\|^2 &\le \|y_m - t\|^2 \\ &\le (1+\theta_m)\|u_m - t\|^2 - \theta_m\|u_{m-1} - t\|^2 + \theta_m(1+\theta_m)\|u_m - u_{m-1}\|^2 \\ &\le \|u_m - t\|^2 + \theta_m[\|u_m - t\|^2 - \|u_{m-1} - t\|^2] + \theta_m(1+\theta_m)\|u_m - u_{m-1}\|^2.\end{aligned}$$

Taking the infimum on both sides, we have

$$\begin{aligned}\inf_{t\in\Gamma} \|u_{m+1} - t\|^2 \le \inf_{t\in\Gamma} \|u_m - t\|^2 &+ \theta_m[\inf_{t\in\Gamma} \|u_m - t\|^2 - \inf_{t\in\Gamma} \|u_{m-1} - t\|^2] \\ &+ \inf_{t\in\Gamma} \theta_m(1+\theta_m)\|u_m - u_{m-1}\|^2.\end{aligned}$$

Let $\aleph_m = \inf_{t\in\Gamma} \|u_m - z\|^2$. Then we can say that

$$\aleph_{m+1} \le \aleph_m + \theta_m(\aleph_m - \aleph_{m-1}) + \chi_m, \tag{3.20}$$

where $\chi_m = \inf_{t\in\Gamma}[\theta_m(1+\theta_m)\|u_m - u_{m-1}\|^2]$. Therefore, we have

$$\begin{aligned}\sum_{m=1}^{\infty} \chi_m &= \textstyle\sum_{m=1}^{\infty} \theta_m(1+\theta_m)\|u_m - u_{m-1}\|^2 \\ &\le \textstyle\sum_{m=1}^{\infty} \theta_m(1+\theta_m)(2M)^2 < \infty.\end{aligned}$$

So, using Lemma 2.6, we have $\beta \in [0, \infty)$ such that $\lim_{m\to\infty} \aleph_m = \beta$ shows that $\lim_{m\to\infty} \inf_{t\in\Gamma} \|u_m - t\|^2$ exists and, therefore, we get $\lim_{m\to\infty} \inf_{t\in\Gamma} \|u_m - t\|$. Using Definition 2.6 and Theorem 3.1(2), we get $\lim_{m\to\infty} \|u_m - \mathcal{K}(u_m)\| = \lim_{m\to\infty} \|u_m - \mathscr{R}_\eta^{\mathcal{J}+\mathscr{M}}(u_m)\| = 0$. Therefore,

$$\lim_{m\to\infty} h(\inf_{t\in\Gamma} \|u_m - t\|) = 0,$$
$$\lim_{m\to\infty} \inf_{t\in\Gamma} \|u_m - t\| = 0.$$

So, there exists a subsequence $\{u_{m_j}\}$ of $\{u_m\}$ and a sequence $\{s_j\}$ satisfying $\|u_{m_j} - s_j\| < \frac{1}{2^j}$. Now we will show that $\{s_j\}$ is a Cauchy sequence. Assume $\epsilon > 0$ and $\lim_{m\to\infty} \inf_{t\in\Gamma} \|u_m - t\| = 0$. There exist $m_0 \in \mathbb{N}$ such that $\inf_{t\in\Gamma} \|u_m - t\| < \dfrac{\epsilon}{6}$ for every $m \geq m_0$. For all $m, n \geq m_0$, we have

$$\|u_n - u_m\| \leq \|u_n - t\| + \|u_m - t\|$$

and

$$\begin{aligned} \|u_n - u_m\| &\leq \inf_{t\in\Gamma} \Big\{\|u_n - t\| + \|u_m - t\|\Big\} \\ &\leq \inf_{t\in\Gamma} \|u_n - t\| + \inf_{t\in\Gamma} \|u_m - t\| \\ &\leq \frac{\epsilon}{6} + \frac{\epsilon}{6} = \frac{\epsilon}{3} \quad \forall m, n \geq m_0. \end{aligned}$$

In addition, there exist $j_0 \in \mathbb{N}$ such that $\frac{1}{2^{j_0}} < \frac{\epsilon}{3}$. Choose $K = \max\{m_0, j_0\}$. Then for all $j > l \geq K$, we obtain

$$\|s_j - s_l\| \leq \|s_j - u_{m_j}\| + \|u_{m_j} - u_{m_l}\| + \|u_{m_l} - s_l\| \leq \epsilon.$$

Therefore, $\{s_j\}$ is a Cauchy sequence that converges to t and Γ is closed, showing that $t \in \Gamma$. Therefore, we can say that $\{u_{m_j}\}$ converges to t and $\lim_{m\to\infty} \inf_{t\in\Gamma} \|u_m - t\|$ exists, so by Theorem 3.1(2), the result follows. □

4. Numerical example

In this section, we will give an example in support of our Theorem 3.1 and show the convergence of our Algorithm 1.

Example 4.1. *Let $\mathcal{X} = \mathbb{R}$ with the usual inner product and let $\mathscr{M} : \mathcal{X} \to 2^{\mathcal{X}}$ be defined by $\mathscr{M}(s) = \{\frac{3}{4}s\}$, $\forall s \in \mathcal{X}$. Then for $\eta = 1$, we calculate the mathematical operator as resolvent operator $\mathcal{R}_{\mathcal{I},\eta}^{\mathscr{M}}$, the Yosida operator $\mathcal{J}_{\mathcal{I},\eta}^{\mathscr{M}}$, and the new resolvent operator $\mathscr{R}_\eta^{\mathcal{J}+\mathscr{M}}$ as*

$$\mathcal{R}_{\mathcal{I},\eta}^{\mathscr{M}}(s) = \frac{4}{7}s, \quad \mathcal{J}_{\mathcal{I},\eta}^{\mathscr{M}}(s) = \frac{3}{7}s, \quad \mathscr{R}_\eta^{\mathcal{J}+\mathscr{M}}(s) = \frac{28}{61}s.$$

We choose $\theta_m = \frac{1}{(m+1)^2}$, $\tau_m = \eta_m = 0.5 + \frac{1}{m}$, $\forall m \geq 1$. We consider two cases for our numerical illustration. In the first case, we set $\varsigma = 0.4$ and define the nonexpansive mapping as $\mathcal{K}(s) = \frac{s}{2}$. In the

second case, we take $\varsigma = 0.1$ *and consider the nonexpansive mapping* $\mathcal{K}(s) = \sin s$. *In both cases, it is easy to verify that* $s = 0 \in \Gamma$ *is a solution of the problem. Using MATLAB 2024b, we plot the graphs for both cases and observe that the sequence* $\{u_m\}$ *converges strongly to* s.

It is straightforward to verify that the assumptions (H1)–(H4) are satisfied. Indeed, since $\theta_m = \frac{1}{(m+1)^2}$, *we have* $\theta_m \in [0, 1]$ *for all* $m \geq 1$ *and* $\sum_{m=1}^{\infty} \theta_m < \infty$, *so (H1) holds. Moreover, the sequences* $\{\tau_m\}$ *and* $\{\eta_m\}$ *are bounded for all* $m \geq 1$, *and hence (H2) is satisfied. Furthermore, for the mappings* $\mathcal{K}(s) = \frac{s}{2}$ *or* $\mathcal{K}(s) = \sin s$, *the sequences* $\{\mathcal{K}(y_m) - y_m\}$ *and* $\{\mathcal{K}(y_m) - s\}$ *are bounded whenever* $\{y_m\}$ *is bounded. Also, since* $\mathscr{R}_1^{\mathscr{J}+\mathcal{M}}(s) = \frac{28}{61}s$, *the sequences* $\{\mathscr{R}_1^{\mathscr{J}+\mathcal{M}}(y_m) - y_m\}$ *and* $\{\mathscr{R}_1^{\mathscr{J}+\mathcal{M}}(y_m) - s\}$ *are bounded whenever* $\{y_m\}$ *is bounded. Thus, conditions (H3) and (H4) are also satisfied.*

The numerical results presented in Table 1 show that the proposed algorithm converges for both cases with initial values $u_0 = 2$ *and* $u_1 = 1.5$. *Case* 1 *shows a faster convergence rate than Case* 2, *reaching a smaller error in fewer iterations. This observation is consistent with the convergence profiles illustrated in Figures 1 and 2, thereby confirming the effectiveness and stability of the proposed method.*

Table 1. Convergence behavior of the proposed algorithm for two cases with initial values $u_0 = 2$ and $u_1 = 1.5$.

Iteration	Case 1	Case 2
0	2	2
1	1.5	1.5
3	0.19996	0.24829
6	0.010316	0.053415
9	0.00058752	0.015102
12	$3.5141e^{-5}$	0.0047003
15	$2.2292e^{-6}$	0.0015395
18	$1.4646e^{-7}$	0.00052051
21	$9.8481e^{-9}$	0.00017986
24	$6.7322e^{-10}$	$6.3142e^{-5}$
30	$3.2551e^{-12}$	$8.0472e^{-6}$

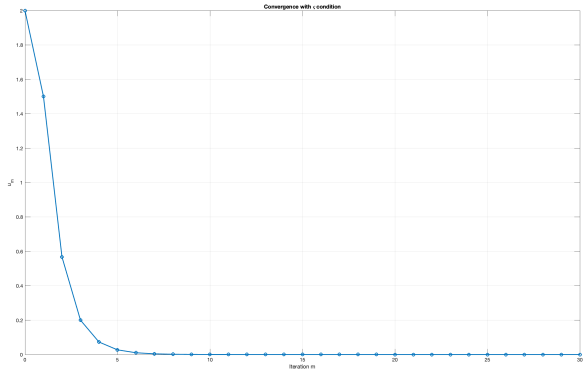

Figure 1. Graphical illustration of the sequence convergence for Case 1.

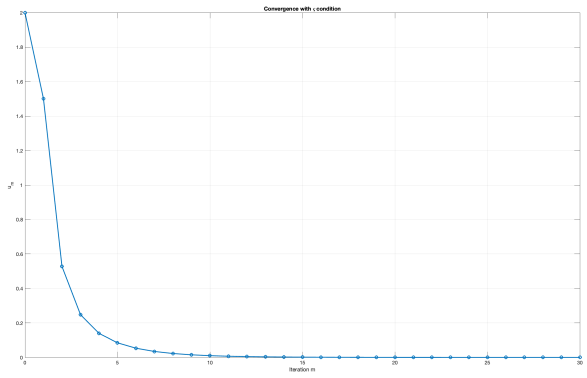

Figure 2. Graphical illustration of the sequence convergence for Case 2.

Example 4.2. *Let $\mathcal{H} = \mathbb{R}^3$ be endowed with the usual inner product*

$$\langle s, t\rangle = s_1t_1 + s_2t_2 + s_3t_3,$$

and the induced norm

$$\|x\| = \sqrt{s_1^2 + s_2^2 + s_3^2},$$

where $x = (s_1, s_2, s_3)$ and $y = (y_1, y_2, y_3)$. Define the mathematical operator $\mathcal{M} : \mathbb{R}^3 \to 2^{\mathbb{R}^3}$ by

$$\mathcal{M}(s_1, s_2, s_3) = \left\{\left(\frac{3}{4}s_1, \frac{1}{2}s_2, \frac{1}{4}s_3\right)\right\}.$$

Clearly, $\mathcal{M}$ is monotone. For $\eta = 1$, the resolvent operator associated with $\mathcal{M}$ is

$$\mathcal{R}^{\mathcal{M}}_{\mathcal{I},\eta}(s_1, s_2, s_3) = \left(\frac{4}{7}s_1, \frac{2}{3}s_2, \frac{4}{5}s_3\right).$$

Using the definition of the Yosida operator, we have

$$\mathcal{J}^{\mathcal{M}}_{\mathcal{I},\eta}(s_1, s_2, s_3) = \left(\frac{3}{7}s_1, \frac{1}{3}s_2, \frac{1}{5}s_3\right).$$

Similarly, we obtain

$$\mathscr{R}^{\mathcal{J}+\mathcal{M}}_{\eta}(s_1, s_2, s_3) = \left(\frac{28}{61}s_1, \frac{6}{11}s_2, \frac{20}{29}s_3\right).$$

Now, we choose

$$\theta_m = \frac{1}{(m+1)^2}, \qquad \tau_m = \eta_m = \frac{1}{2} + \frac{1}{4(m+1)}, \qquad m \geq 1.$$

For the numerical illustration, we consider two cases: the first where $\varsigma = 0.4$ with the nonexpansive mapping

$$\mathcal{K}(s_1, s_2, s_3) = \left(\frac{s_1}{2}, \frac{s_2}{2}, \frac{s_3}{2}\right),$$

and the second where $\varsigma = 0.1$ *with* $\mathcal{K}(s_1, s_2, s_3) = (\sin s_1, \sin s_2, \sin s_3)$. *In both cases, it is easy to verify that* $s = (0, 0, 0) \in \Gamma$ *is a solution of the problem. Using MATLAB 2024b, we plot the graphs for both cases and observe that the sequence* $\{u_m\}$ *converges strongly to* s.

It is straightforward to verify that the assumptions (H1)–(H4) are satisfied. Indeed, since $\theta_m = \frac{1}{(m+1)^2}$, *we have* $\theta_m \in [0, 1]$ *for all* $m \geq 1$ *and* $\sum_{m=1}^{\infty} \theta_m < \infty$, *so (H1) holds. Moreover, the sequences* $\{\tau_m\}$ *and* $\{\eta_m\}$ *are bounded for all* $m \geq 1$, *and hence (H2) is satisfied. Furthermore, for the mappings*

$$\mathcal{K}(x) = \left(\frac{s_1}{2}, \frac{s_2}{2}, \frac{s_3}{2}\right) \text{ or } \mathcal{K}(x) = (\sin s_1, \sin s_2, \sin s_3),$$

the sequences $\{\mathcal{K}(y_m) - y_m\}$ *and* $\{\mathcal{K}(y_m) - s\}$ *are bounded whenever* $\{y_m\}$ *is bounded. Also, since*

$$\mathscr{R}_1^{\mathscr{J}+\mathcal{M}}(s_1, s_2, s_3) = \left(\frac{28}{61}s_1, \frac{6}{11}s_2, \frac{20}{29}s_3\right),$$

the sequences $\{\mathscr{R}_1^{\mathscr{J}+\mathcal{M}}(y_m) - y_m\}$ *and* $\{\mathscr{R}_1^{\mathscr{J}+\mathcal{M}}(y_m) - s\}$ *are bounded whenever* $\{y_m\}$ *is bounded. Thus, conditions (H3) and (H4) are satisfied.*

Using MATLAB 2024b, we plot the graphs for both cases and observe that the sequence $\{u_m\}$ *converges strongly to* $s = (0, 0, 0)$.

The numerical results presented in Table 2 show that the proposed algorithm converges for both cases with initial values $u_0 = (2, 1.5, 1)$ *and* $u_1 = (1.5, 1, 0.5)$ *in* $\mathbb{R}^3$. *Case* 1 *shows a faster convergence rate than Case* 2, *reaching values closer to the solution in fewer iterations. This observation is consistent with the convergence profiles illustrated in Figure 3 and Figure 4, thereby confirming the effectiveness and stability of the proposed method.*

Table 2. Convergence behavior of the proposed algorithm for two cases with initial values $u_0 = (2, 1.5, 1), u_1 = (1.5, 1, 0.5)$.

	Case 1			Case 2		
Iteration	x_1	x_2	x_3	x_1	x_2	x_3
0	2	1.5	1	2	1.5	1
1	1.5	1	0.5	1.5	1	0.5
3	0.19996	0.15794	0.097919	0.24829	0.27314	0.21876
6	0.010316	0.010886	0.010346	0.053415	0.079468	0.09967
9	0.00058752	0.00081552	0.0011654	0.015102	0.028567	0.051462
12	$3.5141e^{-5}$	$6.3652e^{-5}$	0.00013533	0.0047003	0.011074	0.02785
15	$2.2292e^{-6}$	$5.2132e^{-6}$	$1.6258e^{-5}$	0.0015395	0.0044685	0.015452
18	$1.4646e^{-7}$	$4.3936e^{-7}$	$1.9922e^{-6}$	0.00052051	0.0018486	0.0087071
21	$9.8481e^{-9}$	$3.7732e^{-8}$	$2.4728e^{-7}$	0.00017986	0.00077797	0.0049586
24	$6.7322e^{-10}$	$3.2839e^{-9}$	$3.0973e^{-8}$	$6.3142e^{-5}$	0.00033151	0.0028457
30	$3.2551e^{-12}$	$2.5567e^{-11}$	$4.9494e^{-10}$	$8.0472e^{-6}$	$6.1806e^{-5}$	0.00095272

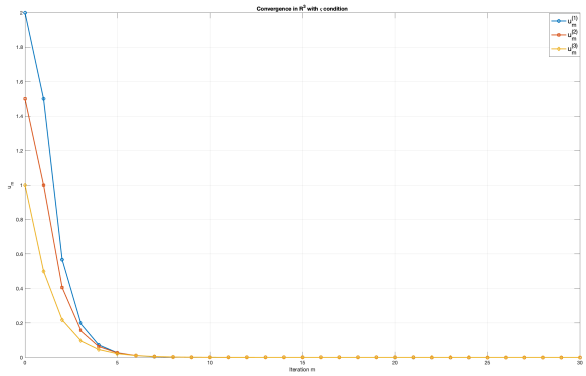

Figure 3. Graphical illustration of the sequence convergence for Case 1.

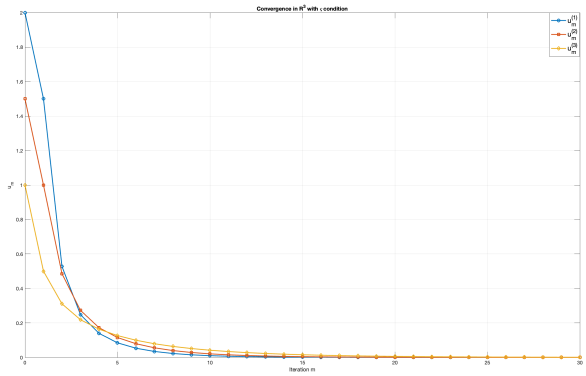

Figure 4. Graphical illustration of the sequence convergence for Case 1.

5. Numerical experiments

In this section, we present numerical experiments to demonstrate the effectiveness of the proposed Algorithm 1 for image restoration problems [20,21]. All experiments were conducted using MATLAB R2021b on a standard desktop computer with an Intel Core i7 processor and 16GB RAM. We used two standard test images from the image processing literature: Cameraman and Moon, both with dimensions of 256×256 pixels. These images were converted to grayscale and normalized to the range $[0, 1]$ to ensure consistent processing across different image sources.

We begin by establishing the precise connection between the image restoration problem and the Yosida inclusion problem introduced in Section 3, so that the subsequent experimental results can be interpreted directly within the theoretical framework of the paper. Let $f \in \mathbb{R}^n$ denote the original image and $g \in \mathbb{R}^n$ the observed degraded image. The image restoration problem seeks to recover f from g under the degradation model

$$g = Kf + \varepsilon, \tag{5.1}$$

where $K : \mathbb{R}^n \to \mathbb{R}^n$ is the blur operator (a 7×7 Gaussian convolution with $\sigma_{\text{blur}} = 2.0$) and ε is additive Gaussian noise with standard deviation $\sigma_{\text{noise}} = 0.05$. A standard variational formulation of

this inverse problem is

$$\min_f \ \frac{1}{2}\|Kf - g\|^2 + \lambda\,\mathrm{TV}(f), \tag{5.2}$$

where $\mathrm{TV}(f) = \|\nabla f\|_1$ is the total variation regularizer promoting piecewise-smooth solutions and $\lambda > 0$ is the regularization parameter. The first-order optimality condition of (5.2) yields the monotone inclusion

$$0 \in K^*(Kf - g) + \lambda\,\partial\,\mathrm{TV}(f), \tag{5.3}$$

where K^* is the adjoint of K and $\partial\,\mathrm{TV}$ denotes the subdifferential of the total variation functional.

To embed (5.3) into the Yosida inclusion problem framework, we define the operator

$$\mathscr{M}(f) \ = \ K^*(Kf - g) + \lambda\,\partial\,\mathrm{TV}(f), \tag{5.4}$$

which is maximal monotone: the gradient term $K^*(K\cdot - g)$ is monotone and Lipschitz continuous with constant $\|K\|^2$, and $\lambda\,\partial\,\mathrm{TV}$ is maximal monotone by the convexity of the total variation functional, so their sum is maximal monotone by Lemma 2.1. With this choice, the optimality condition (5.3) reads simply as $0 \in \mathscr{M}(f)$. The Yosida operator $\mathcal{J}^{\mathscr{M}}_{\mathcal{I},\eta}$ is then constructed from $\mathscr{M}$ via Definition 2.2, and the Yosida inclusion problem (1.4) takes the form

$$0 \in \mathcal{J}^{\mathscr{M}}_{\mathcal{I},\eta}(f) + \mathscr{M}(f). \tag{5.5}$$

The equivalence chain

$$0 \in \mathcal{J}^{\mathscr{M}}_{\mathcal{I},\eta}(f) + \mathscr{M}(f) \iff 0 \in \mathscr{M}(f) \iff 0 \in K^*(Kf - g) + \lambda\,\partial\,\mathrm{TV}(f) \tag{5.6}$$

shows that (5.5) is a concrete instance of the Yosida inclusion problem and that solving it is equivalent to solving the image restoration problem (5.2). The first equivalence in (5.6) follows from the fundamental property of the Yosida approximation: since $\mathcal{J}^{\mathscr{M}}_{\mathcal{I},\eta}(f) = \frac{1}{\eta}(f - \mathcal{R}^{\mathscr{M}}_{\mathcal{I},\eta}(f))$ by Definition 2.2, the inclusion $0 \in \mathcal{J}^{\mathscr{M}}_{\mathcal{I},\eta}(f) + \mathscr{M}(f)$ forces $\mathcal{J}^{\mathscr{M}}_{\mathcal{I},\eta}(f) = 0$, hence $f = \mathcal{R}^{\mathscr{M}}_{\mathcal{I},\eta}(f)$, which by the definition of the resolvent gives $0 \in \mathscr{M}(f)$. The second equivalence is immediate from (5.4).

It remains to specify the nonexpansive mapping $\mathcal{K}$ required by Algorithm 1. Since Algorithm 1 accommodates any nonexpansive mapping, we choose the reflected resolvent

$$\mathcal{K}(f) \ = \ 2\,\mathcal{R}^{\mathscr{M}}_{\mathcal{I},\eta}(f) - f \ = \ 2\,(I + \eta\mathscr{M})^{-1}(f) - f, \tag{5.7}$$

which is nonexpansive because the resolvent $\mathcal{R}^{\mathscr{M}}_{\mathcal{I},\eta}$ is nonexpansive (Lemma 2.1) and the reflection $2T - I$ of any nonexpansive map T is again nonexpansive.

The parameters of Algorithm 1 were set as follows. The inertial weight was chosen as $\theta_m = \frac{1}{(m+1)^2}$, which satisfies condition (H1) since $\sum_{m=1}^{\infty} \theta_m < \infty$ and ensures the inertial contribution diminishes as iterations progress. The convex combination parameters were fixed at $\tau_m = \eta_m = 0.5$ for all m, satisfying condition (H2) with $\varsigma = 0.4$. The proximal parameter was set to $\eta = 1.0$ and the regularization weight to $\lambda = 0.025$, selected via grid search to balance data fidelity and smoothness. The maximum number of outer iterations was 100, and the resolvent subproblem was solved to tolerance 10^{-4} with at most 20 inner iterations.

Under these operator and parameter choices, Algorithm 1 takes the following concrete form for image restoration.

Algorithm 1 (Image Restoration Instance)

Input: degraded image g, blur operator K, parameters $\lambda = 0.025$, $\eta = 1.0$.

Initialize: $u_0 \in \mathbb{R}^n$, $u_{-1} = u_0$, $\theta_m = \frac{1}{(m+1)^2}$, $\tau_m = \eta_m = 0.5$.

For $m = 0, 1, 2, \ldots$, **do:**

Step 1. $y_m = u_m + \theta_m(u_m - u_{m-1})$

Step 2. $z_m = (1 - \tau_m)\, y_m + \tau_m\, (2\, \mathcal{R}^{\mathscr{M}}_{\mathcal{I},\eta}(y_m) - y_m)$

Step 3. $u_{m+1} = (1 - \eta_m)\, (2\, \mathcal{R}^{\mathscr{M}}_{\mathcal{I},\eta}(y_m) - y_m) + \eta_m\, \mathscr{R}^{\mathcal{J}+\mathscr{M}}_{\eta}(z_m)$

Until convergence.

Note that in Step 3, by Lemma 3.1, the resolvent $\mathscr{R}^{\mathcal{J}+\mathscr{M}}_{\eta}$ coincides with $\mathcal{R}^{\mathscr{M}}_{\mathcal{I},\eta}$: a point x satisfies $x = \mathscr{R}^{\mathcal{J}+\mathscr{M}}_{\eta}(v)$ if and only if $0 \in (\mathcal{J}^{\mathscr{M}}_{\mathcal{I},\eta} + \mathscr{M})(x)$, which, as shown in (5.6), is equivalent to $0 \in \mathscr{M}(x)$, i.e., $x = \mathscr{R}^{\mathscr{M}}_{\mathcal{I},\eta}(v)$. Hence both steps reduce to a single resolvent evaluation

$$\mathscr{R}^{\mathscr{M}}_{\mathcal{I},\eta}(v) = (I + \eta\mathscr{M})^{-1}(v),$$

computed at each iteration as

$$\mathscr{R}^{\mathscr{M}}_{\mathcal{I},\eta}(v) \;=\; \arg\min_{u}\Big\{\tfrac{\eta}{2}\,\|Ku - g\|^2 + \tfrac{1}{2}\,\|u - v\|^2 + \eta\lambda\,\mathrm{TV}(u)\Big\}. \tag{5.8}$$

Step 1 applies inertial extrapolation with $\theta_m = \frac{1}{(m+1)^2}$, satisfying (H1). Step 2 forms a convex combination with parameter $\tau_m = 0.5$, and Step 3 combines the two operator evaluations with $\eta_m = 0.5$, both satisfying (H2) with $\varsigma = 0.4$. The resolvent subproblem (5.8) was solved to tolerance 10^{-4} with at most 20 inner iterations. All choices satisfy the hypotheses of Theorem 3.1, so the sequence $\{u_m\}$ converges weakly to a solution of (5.5), equivalently a minimizer of (5.2).

Having established this connection, we now present the experimental results. The test images were degraded using the model (5.1) and Algorithm 1 was run with the parameters described above. We evaluate restoration quality using two standard metrics. The Peak signal-to-noise ratio (PSNR) is defined as

$$\mathrm{PSNR} = 10\log_{10}\left(\frac{\mathrm{MAX}^2}{\mathrm{MSE}}\right)\ (\mathrm{dB}), \tag{5.9}$$

where MAX is the maximum possible pixel value and MSE is the mean squared error between the original and restored images. The Structural similarity index (SSIM) measures perceptual similarity between images, with values in $[0, 1]$, where higher values indicate better structural preservation.

Table 3 presents a summary of the restoration results for both test images. For the Cameraman image, the degradation process reduced the PSNR from the original to 21.20 dB with an SSIM of 0.3397, indicating significant quality loss due to blur and noise. Algorithm 1 successfully restored the image to achieve a PSNR of 23.43 dB and SSIM of 0.7239, demonstrating effective removal of degradation artifacts. The algorithm converged in 23 iterations with a computational time of only 1.01 seconds, showcasing excellent efficiency. Similarly, for the Moon image, the degraded version exhibited a PSNR of 25.71 dB with SSIM of 0.3912, while the restored image achieved 31.56 dB PSNR and 0.7497 SSIM after 35 iterations in 1.77 seconds. These results demonstrate the algorithm's consistent performance across images with different characteristics.

Table 3. Summary of restoration results for Cameraman and Moon images.

Metric	Cameraman		Moon	
	Degraded	Restored	Degraded	Restored
PSNR (dB)	21.20	23.43	25.71	31.56
SSIM	0.3397	0.7239	0.3912	0.7497
Iterations	—	23	—	35
Time (sec)	—	1.01	—	1.77

The improvement metrics presented in Table 4 reveal the substantial enhancement achieved by Algorithm 1. For the Cameraman image, the algorithm achieved a PSNR gain of 2.22 dB, representing a 10.5% relative improvement, with an SSIM improvement of 0.3842. The Moon image demonstrated even more impressive results with a PSNR gain of 5.84 dB (22.7% improvement) and SSIM increase of 0.3585. On average across both test images, Algorithm 1 achieved a 4.03 dB improvement in PSNR and 0.3714 improvement in SSIM, indicating robust and consistent performance regardless of image content. These quantitative results demonstrate that the algorithm is highly effective at removing both blur and noise while preserving important image features and structural information.

Table 4. Improvement metrics for both test images.

Image	PSNR Gain (dB)	SSIM Gain	PSNR Improvement (%)
Cameraman	+2.22	+0.3842	10.5%
Moon	+5.84	+0.3585	22.7%
Average	+4.03	+0.3714	16.6%

Figure 5 presents the complete restoration results for the Cameraman image. The degradation process introduced significant blur and additive Gaussian noise, reducing the PSNR to 21.20 dB and SSIM to 0.3397, with particularly noticeable quality loss in uniform regions and edge details. Algorithm 1 successfully restored the image to achieve a PSNR of 23.43 dB and SSIM of 0.7239, representing an improvement of 2.22 dB. The restored version exhibits sharp edges, reduced noise, and recovered fine details, particularly in the tripod structure, camera body, and photographer's features, demonstrating the algorithm's capability to simultaneously denoise and deblur while maintaining structural integrity.

Figure 5. Cameraman image restoration results using Algorithm 1.

Figure 6 illustrates the convergence behavior of Algorithm 1 for the Cameraman image over 23 iterations. The PSNR evolution shows rapid initial improvement from 21.20 dB to approximately 23 dB within the first 5 iterations, followed by gradual refinement to the final value of 23.43 dB. The logarithmic residual plot demonstrates exponential convergence, with the relative change decreasing from 10^1 to 10^{-3}, confirming the algorithm's stable convergence properties established in Theorem 3.1 via the Yosida approximation framework.

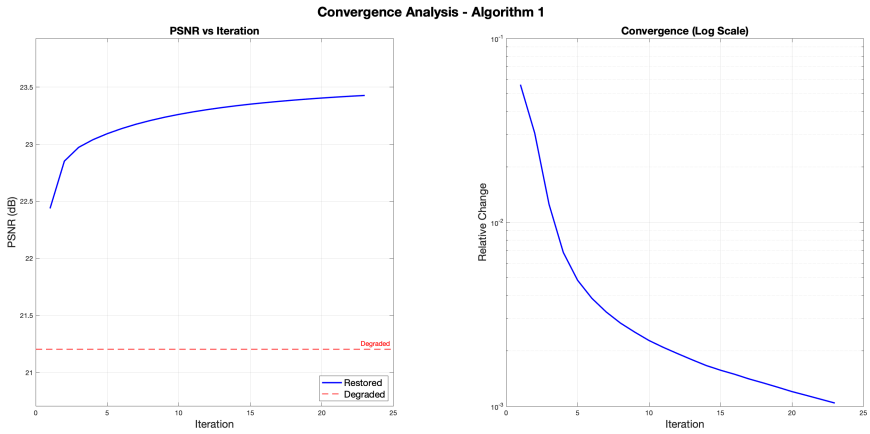

Figure 6. Convergence analysis for Cameraman image restoration.

Figure 7 provides spatial error analysis throughout the restoration process. The degradation error (mean: 0.0355) is concentrated around edges and detailed regions, while the restoration error after applying Algorithm 1 is significantly reduced to 0.0189, distributed uniformly across the image. The error reduction map shows a mean improvement of 0.0166, particularly prominent around edge structures, demonstrating the algorithm's effectiveness across different spatial frequencies without introducing artifacts.

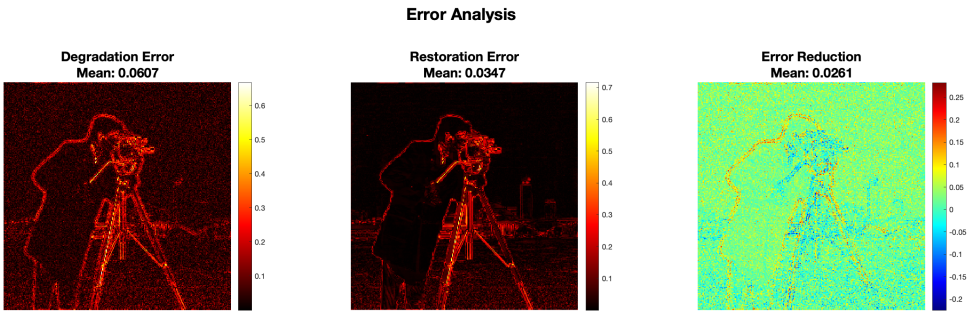

Figure 7. Error analysis for Cameraman image restoration.

Figure 8 presents the restoration results for the Moon image. The degradation process reduced the PSNR to 25.71 dB and SSIM to 0.3912, smoothing crater details and introducing noise across the lunar surface. Algorithm 1 achieved remarkable quality enhancement with a PSNR of 31.56 dB and SSIM of 0.7497, representing a substantial improvement of 5.84 dB. The restored image exhibits

sharpened crater boundaries, recovered surface texture details, and effective noise suppression, with the higher improvement compared to the Cameraman image attributed to the Moon's smoother intensity variations and the correspondingly larger role of Yosida regularization in recovering fine structure from the piecewise-smooth underlying image.

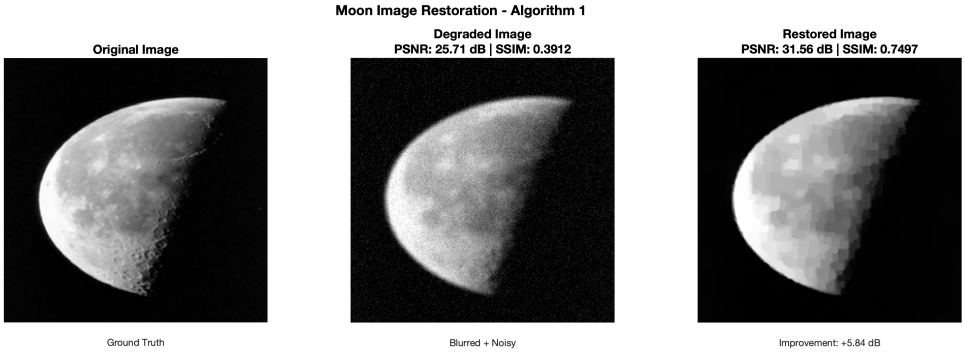

Figure 8. Moon image restoration results using Algorithm 1.

Figure 9 shows the convergence analysis for the Moon image over 35 iterations. The PSNR rapidly improved from 25.71 dB to approximately 30.5 dB within the first 10 iterations and then gradually converged to 31.56 dB. The residual decreased exponentially from 10^{1} to below 10^{-3}, confirming that Algorithm 1 maintains the stable convergence properties guaranteed by the Yosida inclusion framework across different image types.

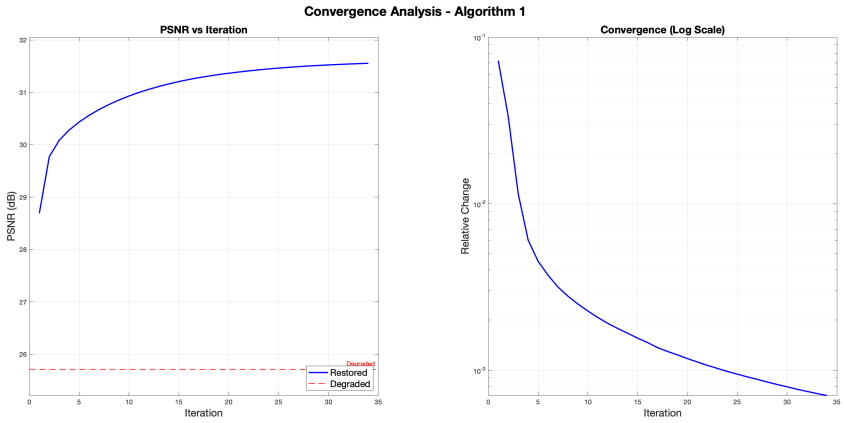

Figure 9. Convergence analysis for Moon image restoration.

Figure 10 presents the error analysis for the Moon image. The degradation error (mean: 0.0607) is distributed uniformly across the lunar surface with higher concentrations around the terminator line and crater edges. After restoration, the error is dramatically reduced to 0.0347, with a mean error reduction of 0.0261, particularly strong along the terminator line and crater regions. The algorithm effectively balances detail preservation with noise suppression across the entire image domain.

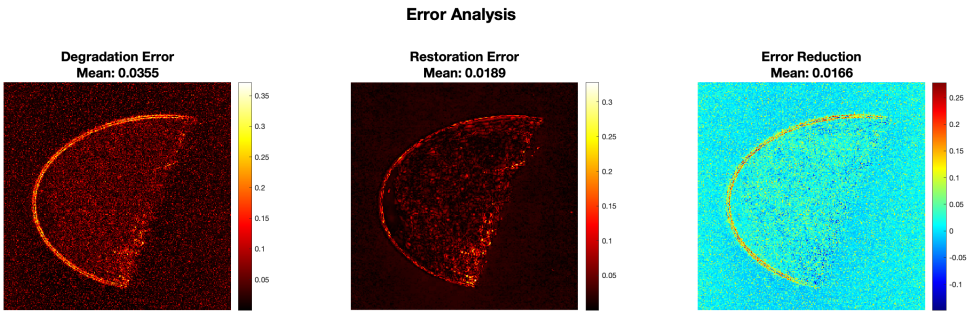

Figure 10. Error analysis for Moon image restoration.

The numerical experiments demonstrate the effectiveness of Algorithm 1 for image restoration and validate the theoretical framework developed in Section 3. The exponential decay of the residual observed in the convergence plots is consistent with the weak convergence guarantee of Theorem 3.1, as the iterative steps, Step 1–Step 3, implement Algorithm 1 with operators $\mathcal{K}$ and $\mathscr{R}_{\eta}^{\mathcal{I}+\mathscr{M}}$ satisfying all required hypotheses. The Cameraman image showed a 2.22 dB improvement in PSNR with SSIM increasing from 0.3397 to 0.7239, while the Moon image demonstrated an even more impressive 5.84 dB gain with SSIM rising from 0.3912 to 0.7497. The average PSNR improvement of 4.03 dB across both images confirms the algorithm's consistent performance regardless of image content.

6. Conclusions

In this work, we proposed an inertial modified S-iteration algorithm for approximating a common solution of a Yosida inclusion problem and a fixed point problem in the setting of real Hilbert space. Under appropriate conditions, we established a weak convergence of the generated sequence to a solution of the proposed problem. Moreover, by imposing additional conditions, strong convergence results were also derived. To validate the theoretical analysis, a numerical example was provided that illustrates the algorithm's convergence behavior. Furthermore, an application to image restoration was presented, demonstrating the effectiveness and applicability of the proposed method in practical inverse problems and supporting the theoretical convergence results. For future research, we plan to investigate the proposed problem using alternative iterative algorithms and extend the present framework to more general spaces such as Banach spaces. Additionally, we aim to explore its applicability to broader classes of nonlinear inclusion and optimization problems, particularly those arising in signal and image processing.

Author contributions

All authors have contributed equally to the work All authors have read and approved the final version of the manuscript for publication.

Use of Generative-AI tools declaration

The authors declare that they have not used Artificial Intelligence (AI) tools in the creation of this article.

Acknowledgments

The Researchers would like to thank the Deanship of Graduate Studies and Scientific Research at Qassim University for financial support (QU-APC-2026).

Conflict of interest

The authors declare that they has no conflict of interest.

References

1. K. Nakajo, W. Takahashi, Strong convergence theorems for nonexpansive mappings and nonexpansive semigroups, *J. Math. Anal. Appl.*, **279** (2003), 372–379.
2. D. Filali, M. Dilshad, M. Akram, M. F. Khan, S. S. Irfan, Hybrid inertial viscosity-type forward-backward splitting algorithms for variational inclusion problems, *AIMS Math.*, **10** (2025), 28829–28860. http://doi.org/10.3934/math.20251269
3. M. Younis, A. H. Dar, N. Hussain, Revised algorithm for finding a common solution of variational inclusion and fixed point problems, *Filomat*, **37** (2023), 6949–6960.
4. P. Tianchi, The zeros of monotone operators for the variational inclusion problem in Hilbert spaces, *J. Inequal. Appl.*, **2021** (2021), 126. https://doi.org/10.1186/s13660-021-02663-2
5. S. Reich, A. Taiwo, Fast hybrid iterative schemes for solving variational inclusion problems, *Math. Methods Appl. Sci.*, **46** (2023), 17177–17198. https://doi.org/10.1002/mma.9494
6. Y. Tang, A. Gibali, Resolvent-free method for solving monotone inclusions, *Axioms*, **12** (2023), 557. https://doi.org/10.3390/axioms12060557 .
7. F. O. Nwawuru, O. K. Narain, M. Dilshad, J. N. Ezeora, Splitting method involving two-step inertial for solving inclusion and fixed point problems with applications, *Fixed Point Theory Algor. Sci. Eng.*, **2025** (2025), 8. https://doi.org/10.1186/s13663-025-00781-w .
8. J. B. Baillon, R. E. Bruck, S. Reich, On the asymptotic behaviour of nonexpansive mappings and semigroups in Banach spaces, *Houst. J. Math.*, **4** (1978), 1–9.
9. M. F. Khan, S. S. Irfan, I. Ahmad, Convergence analysis for system of Cayley generalized variational inclusion on q-uniformly Banach space, *Axioms*, **14** (2025), 361. https://doi.org/10.3390/axioms14050361
10. A. H. Dar, M. K. Ahmad, J. Iqbal, W. A. Mir, Algorithm of common solutions to the Cayley inclusion and fixed point problems, *Kyungpook Math. J.*, **61** (2021), 257–267. https://doi.org/10.5666/KMJ.2021.61.2.257 .
11. S. Husain, M. U. Khairoowala, M. Furkan, Inertial modified S-iteration method for Cayley inclusion problem and fixed point problem, *J. Appl. Math. Comput.*, **70** (2024), 5443–5457. https://doi.org/10.1007/s12190-024-02185-2 .
12. A. Phon-on, N. Makaje, A. Sama-Ae, K. Khongraphan, An inertial S-iteration process, *Fixed Point Theory Appl.*, **2019** (2019), 4. https://doi.org/10.1186/s13663-019-0654-7 .

13. R. Suparatulatorn, W. Cholamjiak, S. Suantai, A modified S-iteration process for G-nonexpansive mappings in Banach spaces with graphs, *Numer. Algor.*, **77** (2018), 479–490. https://doi.org/10.1007/s11075-017-0324-y .
14. H. H. Bauschke, P. L. Combettes, *Convex Analysis and Monotone Operator Theory in Hilbert Spaces*, Berlin: Springer, 2020.
15. M. Dilshad, F. M. Alamrani, A. Alamer, E. Alshaban, M. G. Alshehri, Viscosity-type inertial iterative methods for variational inclusion and fixed point problems, *AIMS Math.*, **9** (2024), 18553–18573. https://doi.org/10.3934/math.2024903
16. H. Brézis, *Opérateurs Maximaux Monotones et Semi-groupes de Contractions Dans Les Espaces de Hilbert*, Amsterdam: Elsevier, 1973.
17. F. Alvarez, Weak convergence of a relaxed and inertial hybrid projection-proximal point algorithm for maximal monotone operators, *SIAM J. Optim.*, **14** (2004), 773–782. https://doi.org/10.1137/S1052623403427859
18. N. Shahzad, R. Al-Dubiban, Approximating common fixed points of nonexpansive mappings in Banach spaces, *Georgian Math. J.*, **13** (2006), 529–537.
19. Q. L. Dong, S. He, Y. J. Cho, A new hybrid algorithm and its numerical realization for two nonexpansive mappings, *Fixed Point Theory Appl.*, **2015** (2015), 150. https://doi.org/10.1186/s13663-015-0399-x
20. T. Goldstein, S. Osher, The split Bregman method for ℓ^1-regularized problems, *SIAM J. Imaging Sci.*, **2** (2009), 323–343. https://doi.org/10.1137/080725891
21. Z. Wang, A. C. Bovik, H. R. Sheikh, E. P. Simoncelli, Image quality assessment: From error visibility to structural similarity, *IEEE Trans. Image Process.*, **13** (2004), 600–612. https://doi.org/10.1109/TIP.2003.819861

Appendix: On the resolvent and Yosida mathematical operator of a maximal monotone operator

Let $\mathscr{M} : \mathcal{X} \to 2^{\mathcal{X}}$ be a maximal monotone operator on a real Hilbert space $\mathcal{X}$, and let $\eta > 0$. The *resolvent* and *Yosida operator* associated with $\mathscr{M}$ are defined, respectively, by

$$\mathcal{R}_{\mathcal{I},\eta}^{\mathscr{M}} = (I + \eta\,\mathscr{M})^{-1}, \qquad \mathcal{J}_{\mathcal{I},\eta}^{\mathscr{M}} = \frac{1}{\eta}\Big(I - \mathcal{R}_{\mathcal{I},\eta}^{\mathscr{M}}\Big).$$

The purpose of this appendix is to establish three properties that collectively justify describing $\mathcal{J}_{\mathcal{I},\eta}^{\mathscr{M}}$ as a *regularized and generically differentiable approximation* of $\mathscr{M}$.

(i) **Single-valuedness and Lipschitz regularity.** Since $\mathscr{M}$ is maximal monotone, the operator $I + \eta\mathscr{M}$ is surjective for every $\eta > 0$, and its inverse $\mathcal{R}_{\mathcal{I},\eta}^{\mathscr{M}}$ is single-valued and defined on all of $\mathcal{X}$. Consequently, $\mathcal{J}_{\mathcal{I},\eta}^{\mathscr{M}}$ is also single-valued and everywhere defined.

Moreover, the resolvent $\mathcal{R}_{\mathcal{I},\eta}^{\mathscr{M}}$ is *firmly nonexpansive*: for all $x, y \in \mathcal{X}$,

$$\left\|\mathcal{R}_{\mathcal{I},\eta}^{\mathscr{M}}(x) - \mathcal{R}_{\mathcal{I},\eta}^{\mathscr{M}}(y)\right\|^2 \leq \left\langle \mathcal{R}_{\mathcal{I},\eta}^{\mathscr{M}}(x) - \mathcal{R}_{\mathcal{I},\eta}^{\mathscr{M}}(y)x - y\right\rangle.$$

In particular, $\mathcal{R}^{\mathscr{M}}_{\mathcal{I},\eta}$ is nonexpansive: $\left\|\mathcal{R}^{\mathscr{M}}_{\mathcal{I},\eta}(x) - \mathcal{R}^{\mathscr{M}}_{\mathcal{I},\eta}(y)\right\| \le \|x - y\|$.

From the definition of $\mathcal{J}^{\mathscr{M}}_{\mathcal{I},\eta}$ and the triangle inequality,

$$\left\|\mathcal{J}^{\mathscr{M}}_{\mathcal{I},\eta}(x) - \mathcal{J}^{\mathscr{M}}_{\mathcal{I},\eta}(y)\right\| \;=\; \frac{1}{\eta}\left\|(x-y) - (\mathcal{R}^{\mathscr{M}}_{\mathcal{I},\eta}(x) - \mathcal{R}^{\mathscr{M}}_{\mathcal{I},\eta}(y))\right\| \;\le\; \frac{1}{\eta}\|x-y\|, \quad \forall\, x, y \in \mathcal{X}.$$

Thus $\mathcal{J}^{\mathscr{M}}_{\mathcal{I},\eta}$ is $\frac{1}{\eta}$-Lipschitz continuous, hence single-valued and globally defined. This stands in sharp contrast to $\mathscr{M}$ itself, which may be multi-valued and discontinuous. In this sense, $\mathcal{J}^{\mathscr{M}}_{\mathcal{I},\eta}$ constitutes a *regularization* of $\mathscr{M}$.

(ii) **Approximation property as $\eta \to 0$.** The term "approximation" refers to the fact that $\mathcal{J}^{\mathscr{M}}_{\mathcal{I},\eta}$ carries precise information about $\mathscr{M}$ and recovers it in the limit $\eta \to 0$. To see this, fix $x \in \mathcal{X}$ and set $p = \mathcal{R}^{\mathscr{M}}_{\mathcal{I},\eta}(x)$. By definition of the resolvent, $x \in p + \eta\,\mathscr{M}(p)$, which gives $(x-p)/\eta \in \mathscr{M}(p)$, and therefore

$$\mathcal{J}^{\mathscr{M}}_{\mathcal{I},\eta}(x) \;=\; \frac{1}{\eta}\Big(x - \mathcal{R}^{\mathscr{M}}_{\mathcal{I},\eta}(x)\Big) \;\in\; \mathscr{M}\Big(\mathcal{R}^{\mathscr{M}}_{\mathcal{I},\eta}(x)\Big).$$

Hence $\mathcal{J}^{\mathscr{M}}_{\mathcal{I},\eta}(x)$ is not merely a heuristic approximation—it is an *exact selection from* $\mathscr{M}$, evaluated at the regularized point $\mathcal{R}^{\mathscr{M}}_{\mathcal{I},\eta}(x)$.

As $\eta \to 0$, one has

$$\left\|\mathcal{R}^{\mathscr{M}}_{\mathcal{I},\eta}(x) - x\right\| \;=\; \eta\,\left\|\mathcal{J}^{\mathscr{M}}_{\mathcal{I},\eta}(x)\right\| \;\to\; 0$$

for bounded $\mathcal{J}^{\mathscr{M}}_{\mathcal{I},\eta}(x)$, so the regularized argument $\mathcal{R}^{\mathscr{M}}_{\mathcal{I},\eta}(x)$ returns to x. Simultaneously,

$$\mathcal{J}^{\mathscr{M}}_{\mathcal{I},\eta}(x) \;\to\; \mathscr{M}^0(x),$$

where $\mathscr{M}^0(x)$ denotes the element of $\mathscr{M}(x)$ with minimal norm. This is the precise sense in which $\mathcal{J}^{\mathscr{M}}_{\mathcal{I},\eta}$ *approximates* $\mathscr{M}$.

(iii) **Generic differentiability.** The Yosida operator is not necessarily Fréchet differentiable at every point in full generality. However, differentiability holds in several natural settings.

Case 1: $\mathscr{M} = \partial f$ with f convex and Fréchet differentiable. In this case, $\mathcal{R}^{\mathscr{M}}_{\mathcal{I},\eta} = \operatorname{prox}_{\eta f}$. When f has a Lipschitz-continuous gradient, the proximal map is Fréchet differentiable, and so is $\mathcal{J}^{\mathscr{M}}_{\mathcal{I},\eta}$, with

$$D\mathcal{J}^{\mathscr{M}}_{\mathcal{I},\eta}(x) \;=\; \frac{1}{\eta}\Big(I - D\operatorname{prox}_{\eta f}(x)\Big).$$

Case 2: $\mathscr{M}$ is single-valued and continuous. When $\mathscr{M}$ itself is single-valued and (locally) Lipschitz continuous, the resolvent is Fréchet differentiable by the implicit function theorem, and differentiability of $\mathcal{J}^{\mathscr{M}}_{\mathcal{I},\eta}$ follows immediately.

Case 3 (General case via Rademacher's theorem). Even without additional smoothness assumptions, when $\mathcal{X} = \mathbb{R}^n$ and $\mathscr{M} = \partial f$ for a convex function f, the map $\mathcal{J}^{\mathscr{M}}_{\mathcal{I},\eta}$ is $\frac{1}{\eta}$-Lipschitz continuous (Part 1) and therefore, by Rademacher's theorem, it is Fréchet differentiable *almost everywhere* with respect to the Lebesgue measure. This is the precise meaning of "generically differentiable" adopted in the abstract.

Illustrative example. Let $\mathcal{X} = \mathbb{R}$ and define $\mathscr{M} : \mathbb{R} \to 2^{\mathbb{R}}$ by $\mathscr{M}(x) = \{ax\}$ for some $a > 0$. This is a single-valued, maximal monotone operator.

Resolvent. Solving $x = p + \eta\, ap = p(1 + \eta a)$ gives

$$\mathcal{R}^{\mathscr{M}}_{\mathcal{I},\eta}(x) \;=\; \frac{x}{1+\eta a}.$$

Yosida operator.

$$\mathcal{J}^{\mathscr{M}}_{\mathcal{I},\eta}(x) \;=\; \frac{1}{\eta}\left(x - \frac{x}{1+\eta a}\right) \;=\; \frac{1}{\eta}\cdot\frac{\eta a\, x}{1+\eta a} \;=\; \frac{ax}{1+\eta a}.$$

Lipschitz constant.

$$\left|\mathcal{J}^{\mathscr{M}}_{\mathcal{I},\eta}(x) - \mathcal{J}^{\mathscr{M}}_{\mathcal{I},\eta}(y)\right| \;=\; \frac{a}{1+\eta a}\,|x-y| \;\le\; \frac{1}{\eta}\,|x-y|,$$

consistent with the bound established in Part 1.

Membership in $\mathscr{M}$.

$$\mathscr{M}\left(\mathcal{R}^{\mathscr{M}}_{\mathcal{I},\eta}(x)\right) \;=\; a\cdot\frac{x}{1+\eta a} \;=\; \mathcal{J}^{\mathscr{M}}_{\mathcal{I},\eta}(x),$$

confirming directly that $\mathcal{J}^{\mathscr{M}}_{\mathcal{I},\eta}(x) \in \mathscr{M}\left(\mathcal{R}^{\mathscr{M}}_{\mathcal{I},\eta}(x)\right)$, as proved in Part 2.

Approximation as $\eta \to 0$.

$$\lim_{\eta\to 0}\mathcal{J}^{\mathscr{M}}_{\mathcal{I},\eta}(x) \;=\; \lim_{\eta\to 0}\frac{ax}{1+\eta a} \;=\; ax \;=\; \mathscr{M}(x).$$

The Yosida operator recovers the original operator in the limit.

Differentiability. The map $x \mapsto ax/(1+\eta a)$ is linear, hence it is Fréchet differentiable everywhere, with constant derivative $a/(1+\eta a)$. This illustrates simultaneously Case 1 and Case 2 of Part 3.

This example concisely demonstrates all three properties established above: $\mathcal{J}^{\mathscr{M}}_{\mathcal{I},\eta}$ is single-valued and Lipschitz continuous (Part 1); it belongs to $\mathscr{M}$ at a regularized argument and converges to $\mathscr{M}$ as $\eta \to 0$ (Part 2); and it is everywhere differentiable (Part 3).